

Time Dependence of Spin Operators in Finite Heisenberg Linear Chains*

FERNANDO CARBONI† AND PETER M. RICHARDS

Department of Physics, University of Kansas, Lawrence, Kansas 66044

(Received 12 July 1968)

Numerical calculations of quantum-mechanical time correlation functions are reported for finite Heisenberg linear chains containing up to 10 spin- $\frac{1}{2}$ particles. The results, obtained by manipulation of eigenvalues and eigenfunctions, give Fourier transforms in histogram form. Two-spin correlation functions show a sharp rise near zero frequency and highly non-Gaussian behavior at infinite temperature. The short-time behavior is estimated and compared with classical calculations and other theories. Four-spin functions are calculated and compared with results of a simple decoupling approximation. Spatial Fourier transforms of two-spin functions as needed for neutron scattering cross sections are computed. These are limited to fairly short wavelengths by the finiteness of the system. The temperature dependence of two-spin functions shows a decrease in the near-zero frequency component with decreasing temperature. Computed correlation functions are used to predict the frequency dependence of the ESR linewidth in the linear-chain salt $\text{Cu}(\text{NH}_3)_4\text{SO}_4 \cdot \text{H}_2\text{O}$, and comparison is made with experiment. Very good agreement is found using the same exchange constant J as inferred from specific-heat and magnetic-susceptibility data. The Gaussian approximation, on the other hand, is in extremely poor agreement.

I. INTRODUCTION

PROPERTIES of the Heisenberg linear chain have received considerable attention in recent years. The linear chain Hamiltonian for N particles given by

$$\mathcal{H}_{\text{ex}} = 2J \sum_{i=1}^N \mathbf{S}_i \cdot \mathbf{S}_{i+1}, \quad (1)$$

where J is the isotropic exchange interaction coupling nearest-neighbor spins \mathbf{S}_i and \mathbf{S}_{i+1} on lattice sites i and $i+1$, respectively, has been solved exactly in the limit $N \rightarrow \infty$ for the antiferromagnetic ($J > 0$) ground-state energy.¹⁻⁴ With high-speed computers it has been possible^{5,6} to obtain eigenvalues for closed ($\mathbf{S}_{N+1} = \mathbf{S}_1$) chains containing up to $N=11$ spin- $\frac{1}{2}$ particles. Bonner and Fisher⁶ have made a particularly thorough investigation of thermodynamic properties in finite chains and showed that the ground-state energy versus N extrapolates to within 0.1% of the correct value for $N = \infty$.

The Heisenberg linear chain has more than mathematical interest since there exist paramagnetic salts which exhibit magnetic properties which can nearly be described by (1). This occurs as a result of magnetic ions being arranged in linear chains parallel to a fixed crystal direction and with intrachain exchange interactions very much greater than interchain coupling, as illustrated in Fig. 1. One of the best documented linear chain materials is $\text{Cu}(\text{NH}_3)_4\text{SO}_4 \cdot \text{H}_2\text{O}$ (referred

to hereafter as CTS). Griffiths⁷ has applied Bonner and Fisher's results to CTS and showed that its specific heat and magnetic susceptibility conform to a linear chain with $J/k = 3.15^\circ\text{K}$ (k is Boltzmann's constant).

Although static (thermodynamic) properties have been computed for finite linear chains, no such computation of time-dependent properties had been performed prior to this work in which we have treated closed chains with $N=10$ and fewer and open chains with $N=9$ and fewer. The time-dependent quantities of interest here are two-spin and four-spin correlation functions $\langle S_i^\alpha(t) S_j^\beta(0) \rangle$ and $\langle S_i^\alpha(t) S_j^\beta(t) S_k^{\alpha'}(0) S_l^{\beta'}(0) \rangle$, where $S_i^\alpha(t)$ is the α th component of the spin at lattice site i at time t and the triangular brackets stand for thermal average. These quantities are directly related to neutron scattering cross sections and exchange-narrowed magnetic resonance so that in principle there could be as much experimental interest in time correlation functions as in static correlations. Neutron scattering provides the most direct measurement of two-spin time-correlation functions since the differential scattering cross section is given by^{8,9}

$$d\sigma/d\Omega d\omega \propto \sum_{ij} \int_{-\infty}^{\infty} dt \langle \mathbf{S}_{i\perp}(t) \cdot \mathbf{S}_{j\perp}(0) \rangle e^{i\omega t} e^{i\mathbf{q} \cdot \mathbf{r}_{ij}}, \quad (2)$$

where $d\sigma/d\Omega d\omega$ is the cross section for scattering with a change of neutron momentum $\hbar\mathbf{q}$ and energy $\hbar\omega$, and $\mathbf{S}_{i\perp}$ is the component of \mathbf{S}_i perpendicular to \mathbf{q} . To our knowledge, though, no experiments have as yet been performed on linear chain systems which would serve as a detailed test for the correlation functions calculated here.

Exchange-narrowed magnetic-resonance linewidth is

* Supported in part by the United States Atomic Energy Commission. Brief accounts of portions of this work have been published in *J. Appl. Phys.* **39**, 967 (1968) and Ref. 11.

† Present address: Department of Physics, University of Costa Rica, San Jose, Costa Rica.

¹ H. A. Bethe, *Z. Physik* **71**, 205 (1931).

² L. Hulthein, *Arkiv Mat. Astron. Fysik* **26A**, No. 11 (1938).

³ R. L. Orbach, *Phys. Rev.* **112**, 309 (1958).

⁴ L. R. Walker, *Phys. Rev.* **116**, 1089 (1959).

⁵ R. L. Orbach, *Phys. Rev.* **115**, 1181 (1959).

⁶ J. C. Bonner and M. E. Fisher, *Phys. Rev.* **135**, A640 (1964).

⁷ R. B. Griffiths, *Phys. Rev.* **135**, A659 (1964).

⁸ L. Van Hove, *Phys. Rev.* **95**, 1374 (1954).

⁹ P. G. de Gennes, in *Magnetism*, edited by G. T. Rado and H. Suhl (Academic Press Inc., New York, 1963), Vol. III, p. 115.

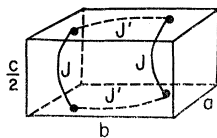


FIG. 1. $\text{Cu}(\text{NH}_3)_4\text{SO}_4 \cdot \text{H}_2\text{O}$ (CTS) lattice. One half the orthorhombic unit cell is shown together with position of Cu^{++} ions (\bullet). Superexchange through intermediate ions (not shown) is believed to give rise to $J \gg J'$, where J is exchange interaction between nearest neighbor Cu^{++} ions on a given chain parallel to c axis and J' is the interchain coupling. Lattice of Cu^{++} ions is orthorhombic C with constants a , b , $\frac{1}{2}c$. $a=7.07 \text{ \AA}$, $b=12.12 \text{ \AA}$, $c=10.16 \text{ \AA}$.

related¹⁰ to combinations of four-spin time-correlation functions for the most common case of broadening due to dipolar interactions. Precise formulas are given in Sec. IV. Although the relationship between linewidth and correlation functions is not as simple as in the neutron case (2), it is possible to predict frequency dependence of linewidth in linear chain materials from our results; and experimental data do exist^{11,12} with which comparison can be made. As shown in Sec. IV and discussed in a previous publication,¹² agreement between theory and experiment on this point is entirely satisfactory.

An original motivation for undertaking this work was the lack of agreement for CTS between experiment¹¹ and the Gaussian approximation for time-correlation functions. By Gaussian approximation we mean the following: The general time correlation function $\langle A(t)B(0) \rangle$ may be expanded in powers of t according to

$$\langle A(t)B(0) \rangle = \langle AB \rangle + \frac{1}{2}t^2 \langle [\mathcal{H}C, [\mathcal{H}C, A]] B \rangle + \dots, \quad (3)$$

in which time dependence of A is given in the Heisenberg picture by

$$A(t) = e^{i\mathcal{H}t/\hbar} A e^{-i\mathcal{H}t/\hbar}, \quad (4)$$

and we have assumed the linear term in t to vanish (as it does at infinite temperature for the spin operators of interest here). In practice it is exceedingly difficult to carry the expansion in (3) beyond terms in t^4 ; so some analytic form for $\langle A(t)B(0) \rangle$ must be assumed in order to perform Fourier frequency transforms. Gaussian decay has received the most attention^{10,13} whereby (3) is written as

$$\langle A(t)B(0) \rangle = \langle AB \rangle e^{-\omega_e^2 t^2/2} \quad (5a)$$

with

$$\omega_e^2 = -\langle [\mathcal{H}C, [\mathcal{H}C, A]] B \rangle / \langle AB \rangle. \quad (5b)$$

Equations (5), of course, in no way prove the decay to be Gaussian; they merely say that *if* the form is Gaus-

sian then the single parameter ω_e is uniquely determined. It may be argued that if the short-time expansion (3) has any meaning, then the correlation can be expected to decay with a characteristic time close to ω_e^{-1} even though the function may not be precisely Gaussian.

Application of the above reasoning to CTS gives a frequency dependence of electron-spin-resonance linewidth characterized by ω_e . That is, when the resonance angular frequency ω equals ω_e , the linewidth should be roughly halfway between its values for $\omega \rightarrow 0$ and $\omega \rightarrow \infty$. Analysis of data in this manner together with an appropriate relation between ω_e and J which may be derived from (1) and (3) lead Rogers *et al.*¹¹ to conclude $J/k=0.5^\circ\text{K}$ for CTS, whereas specific heat and susceptibility data⁷ suggest $J/k=3.15^\circ\text{K}$; so a serious discrepancy was apparent for the linear chain system, and it was clearly of interest to see whether exact calculations could resolve the difficulty. An affirmative answer definitely seems to have been obtained, as we show here and elsewhere.¹² For three-dimensional systems, the Gaussian approximation seems to be at least roughly correct since measurements on frequency dependence of linewidth^{14,15} in such substances give values of J in reasonable agreement with specific heat and susceptibility studies.

Recent attempts have been made by various authors to improve upon the crude Gaussian approximation (5). However, it seems that although general integro-differential equations may be derived, a Gaussian or similar assumption must be invoked at some stage of the calculation in order to obtain even approximate solutions.^{16,17} The approach here is basically different in that an exact *ab initio* calculation is made of $\langle A(t)B(0) \rangle$ starting from the quantum-mechanical definition (4)

$$\langle A(t)B(0) \rangle = \sum_{\mu\nu} A_{\mu\nu} B_{\nu\mu} e^{i\omega_{\mu\nu}t} P_{\mu}, \quad (6)$$

where

$$\hbar\omega_{\mu\nu} = E_{\mu} - E_{\nu}, \quad (7)$$

and

$$P_{\mu} = e^{-E_{\mu}/kT} / \sum_{\nu} e^{-E_{\nu}/kT}, \quad (8)$$

in which E_{μ} is the energy of the eigenstate Φ_{μ} of the Hamiltonian and $A_{\mu\nu}$ is the matrix element $\langle \Phi_{\mu} | A | \Phi_{\nu} \rangle$. It is possible to get a meaningful description of, for example, $\langle S_x^z(t) S_x^z(0) \rangle$ from (6) for finite closed chains containing six or more spins because we expect at high temperatures a cluster of spins containing up to third nearest neighbors of the spin of interest to give a reasonable approximation. A cluster containing up to

¹⁰ R. Kubo and K. Tomita, J. Phys. Soc. Japan **9**, 888 (1954).

¹¹ R. N. Rogers, F. Carboni, and P. M. Richards, Phys. Rev. Letters **19**, 1016 (1967).

¹² R. N. Rogers, J. K. Pribram, and R. D. Lazay, Bull. Am. Phys. Soc. **9**, 740 (1964).

¹³ P. W. Anderson and P. R. Weiss, Rev. Mod. Phys. **25**, 269 (1953).

¹⁴ A. J. Henderson and R. N. Rogers, Phys. Rev. **152**, 218 (1966).

¹⁵ R. C. Richardson, A. Landesman, E. Hunt, and H. Meyer, Phys. Rev. **146**, 244 (1966).

¹⁶ H. Bennet and P. C. Martin, Phys. Rev. **138**, 607 (1965).

¹⁷ M. De Leener and P. Resibois, Phys. Rev. **152**, 318 (1966).

third nearest neighbors would contain a prohibitive number of spins for two- and three-dimensional lattices; so our methods seem to be restricted to linear chains, at least with present day computers.

An exact numerical calculation is also useful from a general theoretical standpoint since it can be an aid in evaluating various approximations. Wherever possible, we therefore compare our results with published theories of time dependence in Heisenberg paramagnets, as well as with experiment.

A major computational difference between this work and previous studies of finite linear chains is that here eigenfunctions are necessary as well as eigenvalues. Thermodynamic properties, of course, require only eigenvalues.

An outline of this paper is as follows. Calculation procedures are discussed in Sec. II. Results are presented and discussed in Sec. III under the subheadings (A) Density of States, (B) Two-Spin Correlation Functions, (C) Wave-Vector Representation of Two-Spin Correlations [i.e., formulation appropriate to neutron-scattering cross sections (2)], (D) Four-Spin Correlation Functions and Decoupling, and (E) Temperature Dependence. The results of Sec. III are applied in Sec. IV to a detailed calculation of frequency dependence of electron-spin-resonance linewidth in CTS. Section V contains a summary and conclusions. In the Appendix a derivation is given of a numerical notation for the basis functions whereby it is possible to have the computer generate the states and matrix elements. This method eliminates all tedious hand calculations preliminary to matrix diagonalization by the computer.

II. CALCULATION

Computation of eigenvalues and eigenfunctions associated with the Hamiltonian (1) for closed chains is performed in a manner similar to that discussed in Refs. 5 and 6. As in these references, the original $2^N \times 2^N$ matrix is reduced to considerably smaller diagonal blocks by using eigenfunctions of the total z component of spin S_z and combinations of the translation operator τ (see the Appendix). A further reduction is possible for states with $S_z=0$ since then a rotation operator R which reverses direction of each spin may be used. (Obviously, R commutes with S_z only for $S_z=0$, so it is useful only in this case.) Since eigenvalues of τ are complex, we have found it necessary to work too with eigenfunctions¹⁸ of $\tau+\tau^*$ in order to obtain real, symmetric matrices for which subroutines exist for eigenfunctions and eigenvalues. The largest matrix which need be diagonalized for $N=10$ is then 44×44 .

Open chains of up to nine spins have also been considered. Here translational invariance is lost, so

¹⁸ Details of use of the translation operator and other features of the calculation may be found in F. Carboni, Ph.D. thesis, University of Kansas, 1967 (unpublished).

the matrices are much larger. Reflection symmetry about the midpoint can be used, however, to reduce the order of a given S_z matrix by about a factor of 2. In this way the largest matrix to be diagonalized for $N=9$ is 66×66 .

The limiting factor on the number of spins treated is the manipulation required by (6) rather than matrix diagonalization. This is because an individual spin component S_i^α does not commute with the translation operator, so that $\langle \Phi_\mu | S_i^\alpha | \Phi_\nu \rangle$ is in general nonzero even if Φ_μ and Φ_ν are eigenfunctions with different eigenvalues of τ . Thus the full matrix for a given S_z , which is as large as 252×252 for $N=10$, must be considered in computing-time correlations.

A novel feature of the calculation is use of a numerical notation for the basis functions. This method, described in the Appendix, allows the computer to generate the basis functions for a given S_z , from eigenfunctions of τ , and take matrix elements of \mathcal{H}_{ex} or any other set of spin operators. Tedious hand calculation of matrix elements is completely eliminated in this way, and with our program essentially the only input datum is the number of spins on the chain.

Eigenvalues and eigenfunctions were checked and found to agree with results of previous workers^{5,6} wherever comparison was possible. Time correlations were checked as described in Sec. III.

Most calculations were performed on an IBM 7040. Results for 10 spins and open chains were obtained with a GE 625 which became available after the bulk of this work was completed. An idea of the relative difficulties of diagonalization and computation of correlation functions may be obtained from the fact that eigenfunctions and eigenvalues were computed for up to $N=11$ on the IBM 7040; but only with the much faster and larger core GE 625 was it feasible to calculate time-correlation functions for $N=10$ (running time 6 h, not including time for diagonalization) and $N=11$ was felt to be out of the question even with this machine.

III. RESULTS AND DISCUSSION

Results are in the form of histograms for the Fourier transform of a given time-correlation function defined as follows: In the basic expression (6) we collect all terms $\omega_{\mu\nu}$ which lie in the interval

$$\omega_n - \frac{1}{2}\Delta\omega \leq \omega_{\mu\nu} < \omega_n + \frac{1}{2}\Delta\omega,$$

so that we define

$$\tilde{f}(\omega_n) = \frac{1}{\Delta\omega} \sum_{\mu\nu} A_{\mu\nu} B_{\nu\mu} P_{\mu} \zeta(\omega_{\mu\nu} - \omega_n), \quad (9)$$

where

$$\zeta(\omega_{\mu\nu} - \omega_n) = \begin{cases} 1 & \text{if } \omega_n - \frac{1}{2}\Delta\omega \leq \omega_{\mu\nu} < \omega_n + \frac{1}{2}\Delta\omega \\ 0 & \text{otherwise.} \end{cases} \quad (10)$$

Values of interval centers ω_n are chosen so that the

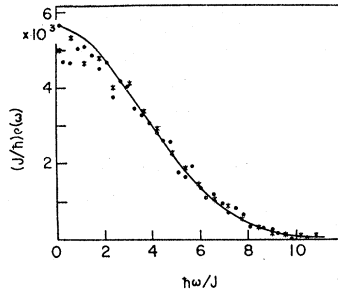


FIG. 2. Density of states $\rho(\omega)$ for closed chain of 9 spins. Solid curve is $(J/\hbar)\rho(\omega) = 5.6 \times 10^3 \exp(-\omega^2/\Omega^2)$ with $\Omega = 5J/\hbar$. \bullet , $\Delta\omega = 0.3J/\hbar$; $*$, $\Delta\omega = 0.6J/\hbar$.

n th interval is centered at $n\Delta\omega$ with $n = 0, \pm 1, \pm 2 \dots$. The quantity $\tilde{f}(\omega_n)$ is then related to the continuous function (assuming a continuous distribution of frequencies) $f(\omega)$ by

$$\tilde{f}(\omega_n) = \frac{1}{\Delta\omega} \int_{\omega_n - \Delta\omega/2}^{\omega_n + \Delta\omega/2} f(\omega) d\omega. \quad (11)$$

We shall henceforth not make a sharp distinction between $\tilde{f}(\omega_n)$ and $f(\omega)$ but often refer simply to $f(\omega)$ with the understanding that $\tilde{f}(\omega_n)$, the average of $f(\omega)$ within a given interval, is the quantity actually calculated.

A check on validity of the $\tilde{f}(\omega_n)$ is that if

$$\langle A(t)B(0) \rangle = \int_{-\infty}^{\infty} d\omega f(\omega) e^{i\omega t}, \quad (12)$$

then

$$\langle AB \rangle = \int_{-\infty}^{\infty} d\omega f(\omega) = \sum_n \tilde{f}(\omega_n) \Delta\omega. \quad (13)$$

Since $\langle AB \rangle$ is readily obtained, at least at infinite temperature, Eq. (13) provides a convenient test to which all calculated $f(\omega_n)$ were subjected. Agreement was obtained to within four significant figures.

Choice of the interval $\Delta\omega$ is governed by considering that if $\Delta\omega$ is too small irregular oscillations appear due to the discrete nature of the calculations, while if $\Delta\omega$ is too large, information as to frequency dependence is lost. It was found that at infinite temperature $\Delta\omega = 0.8J/\hbar$ gave histograms through which reasonably smooth curves could be drawn for chains with $N \geq 6$. In some cases we also present results for narrower intervals. At lower temperatures several oscillations occur even with $\Delta\omega = 0.8J/\hbar$, and we have much less confidence that the low-temperature results are representative of the infinite chain [see (E) of this section]. For this reason most of the discussion will be limited to infinite temperature. Unless stated otherwise, all results presented below are for infinite temperature and closed chains.

A. Density of States

The density of states $\rho(\omega)$ is defined by

$$\rho(\omega) = \frac{1}{\Delta\omega} \sum_{\mu\nu} \zeta(\omega_{\mu\nu} - \omega), \quad (14)$$

so that it represents the average number of states within the interval $\Delta\omega$. It is shown in Fig. 2 both for $\Delta\omega = 0.3J/\hbar$ and $\Delta\omega = 0.6J/\hbar$ with $N = 9$. The smoothing effect of interval widening is apparent. A Gaussian

$$\rho(\omega) = \rho(0)e^{-\omega^2/\Omega^2} \quad (15)$$

with $\Omega = 5J/\hbar$ gives a good fit. This is particularly interesting in view of the steep rise near zero frequency exhibited by the correlation functions [Sec. (B)]. It means that any divergence of a correlation function near zero frequency must be associated with the matrix elements themselves being heavily weighted in favor of zero-frequency transitions rather than an anomaly in the density of states.

B. Two-Spin Correlation Functions

Two-spin correlations are given by the function $f_j(\omega)$ defined by

$$\langle S_i^z(t) S_{i+j}^z(0) \rangle = \int_{-\infty}^{\infty} d\omega f_j(\omega) e^{i\omega t}. \quad (16)$$

Plots of $f_j(\omega)$ for $j = 0-4$ are shown in Figs. 3 and 4 for $N = 10$. A histogram is presented in Fig. 3 while, for simplicity, the other figures show points taken at interval centers. The function $f_j(\omega)$ passes through zero j times. This feature is readily understood from the short-time behavior. At infinite temperature we have

$$\left. \frac{d^{2n}}{dt^{2n}} \langle S_i^z(t) S_{i+j}^z(0) \rangle \right|_{t=0} = 0 \quad \text{for } n < j,$$

so that the moments

$$\int_{-\infty}^{\infty} \omega^{2n} f_j(\omega) d\omega = 0 \quad \text{for } n < j,$$

and, hence, as j increases the number of zeros of $f_j(\omega)$ must increase so as to accommodate more zero moments.

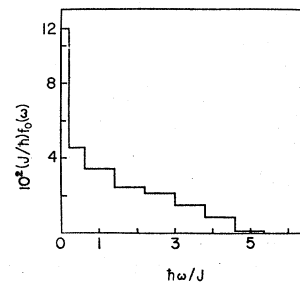


FIG. 3. Histogram of two-spin self-correlation function $f_0(\omega)$ for closed chain, $N = 10$.

The most noteworthy feature is that all $f_j(\omega)$ show a sharp rise near zero frequency. Fernandez and Gersch¹⁹ have suggested that all $f_j(\omega)$ should diverge at least logarithmically as $\omega \rightarrow 0$ for a one-dimensional Heisenberg linear chain, and Griffiths²⁰ has demonstrated logarithmic divergence for a linear chain in which interaction is between transverse components of spin (X - Y model) only. If $\langle S_i^z(t)S_i^z \rangle$ is spatially Fourier-

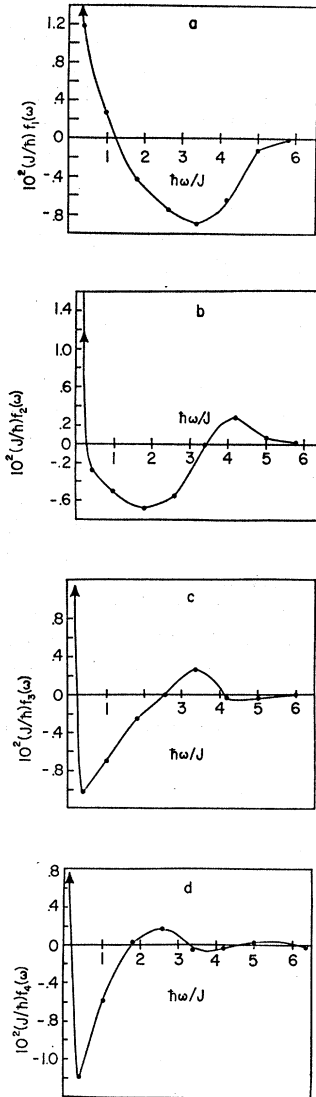


FIG. 4. Two-spin correlation functions $f_j(\omega)$ for $j=1$ (nearest neighbors) to $j=4$ (fourth nearest neighbors). Closed chain, $N=10$. Points are taken at centers of histogram intervals for same frequency intervals as shown in Fig. 3. Points for interval centered at $0.1J/\hbar$ are not displayed. Their values on vertical scale are as given below: (a) $f_1(\omega)$; point at $0.1J/\hbar=7.8$, (b) $f_2(\omega)$; point at $0.1J/\hbar=6.2$, (c) $f_3(\omega)$; point at $0.1J/\hbar=5.1$, (d) $f_4(\omega)$; point at $0.1J/\hbar=4.5$.

¹⁹ J. F. Fernandez and H. A. Gersch Phys. Rev. **172**, 341 (1968).

²⁰ R. B. Griffiths (private communication).

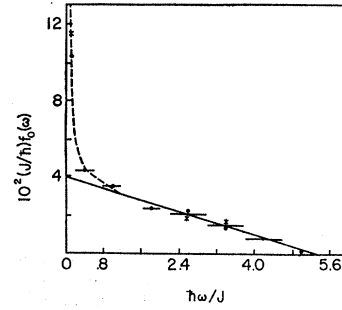


FIG. 5. Self-correlation function $f_0(\omega)$ extrapolated to $N=\infty$. Horizontal lines represent width of frequency interval. \bullet , extrapolation for closed chains; $*$, extrapolation for open chains. Where only \bullet is shown, difference between open and closed chain extrapolations is too small to show on graph. Solid line is $(J/\hbar)f_0(\omega) = 0.04[1 - \hbar\omega/5.28J]$. Dashed curve is meant only as aid to the eye.

analyzed according to

$$\langle S_i^z(t)S_i^z \rangle = N^{-1} \sum_q \langle S_q^0(t)S_{-q}^0 \rangle \quad (17)$$

with

$$S_q^0 = N^{-1/2} \sum_i e^{iqx_i} S_i^z, \quad (18)$$

and it is assumed that long-wavelength modes obey a diffusion equation, then an $\omega^{-1/2}$ divergence results. Any divergence less severe than ω^{-1} satisfies the sum rule

$$\int_{-\infty}^{\infty} d\omega f_0(\omega) = \frac{1}{4} \quad (19)$$

so diffusive modes in the linear chain are allowable. No divergence is expected in three dimensions on the basis of this argument. Our computed $f_j(\omega)$ strongly suggest a divergence as $\omega \rightarrow 0$, but the intervals $\Delta\omega$ are far too "coarse grained" for us to say anything about the nature of the divergence or even, in fact, whether or not a true divergence exists.

The self-correlation function $\langle S_i^z(t)S_i^z(0) \rangle$, whose transform is $f_0(\omega)$, is of particular interest. It is likely to be the function for which finite-chain calculations give the most reasonable extrapolation to $N=\infty$ since it involves shorter-range correlations. Also, among the two-spin correlation functions, it is the only one which is nonzero at $t=0$ (for infinite temperature) and thus the only one for which a Gaussian approximation might make any sense. We have therefore paid special attention to $f_0(\omega)$ and made an extrapolation to $N=\infty$ in the following manner. For each frequency interval we plot $f(\omega)$ versus some power of $1/N$ for $N=6-10$, with closed chains and $N=6-9$ with open chains [for open chains i in S_i^z is taken to be $\frac{1}{2}N$ for N even and $\frac{1}{2}(N+1)$ for N odd]. This is similar to the method used by Bonner and Fisher for showing that the known antiferromagnetic ground-state energy can be extrapolated

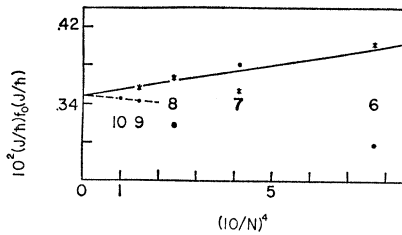


FIG. 6. Self-correlation function $f_0(\omega)$ in interval $0.6J/\hbar \leq \omega < 1.4J/\hbar$ for varying N , as shown by numbers in vicinity of points. ●, closed chains; *, open chains. This is a particularly good example of where a reliable extrapolation can seem to be made because—apart from $N=7$ —there is a general upward trend for closed chains and downward trend for open chains; and these trends can be extrapolated to a common point at $1/N=0$, as given by intersecting lines.

olated too from finite-chain calculations. They found a plot versus $1/N^2$ to give a straight line. In our case, a plot versus $1/N^4$ yields the closest to a straight line in most cases. Extrapolation is, of course, based on the premise that nothing catastrophic occurs beyond $N=10$ to change completely the trend with increasing N . Since the temperature is infinite and this is a one-dimensional system, we are doubly insured against long-range order effects and therefore expect extrapolations to be reasonable. For the worst cases considered, there is no more than a 10% deviation between the extrapolated value and the point for the maximum N calculated.

Separate extrapolations were made for open and closed chains. In general the open chains showed smaller variation with N than closed chains. Figure 5 gives the resulting $f_0(\omega)$ extrapolated to $N=\infty$. Only for the lowest-frequency interval, centered at $0.1J/\hbar$, is the difference between open- and closed-chain extrapolations significant. Two extrapolation curves are given in Figs. 6 and 7. These represent, respectively, the best and worst examples in terms of a regular variation with N .

For $\omega > J/\hbar$ a triangular distribution $0.04(J/\hbar)^{-1} \times (1 - \hbar\omega/5.28J)$ is a satisfactory fit as shown by the straight line in Fig. 5. The complete curve $f_0(\omega)$ is then described by this distribution plus a function which diverges as $\omega \rightarrow 0$ at a rate faster than or equal to $\ln(1/\omega)$ but slower than $1/\omega$ and which goes to zero for $\omega \lesssim J/\hbar$. Calling this divergent function $\eta(\omega)$, we have

$$f_0(\omega) = 0.04(J/\hbar)^{-1}(1 - \hbar\omega/5.28J) + \eta(\omega), \quad \omega \leq 5.28J/\hbar$$

$$= 0, \quad \omega > 5.28J/\hbar. \quad (20)$$

The cut off in the vicinity of $5J/\hbar$ is particularly striking. We are fairly confident that it is not due to the finiteness of the system since the cutoff interval is independent of N for $N \geq 6$. This feature rules out a Gaussian behavior even for high frequencies. The Fourier transform of (20) gives [$f_0(-\omega) = f_0(\omega)$ at infinite temperature]

$$\langle S_i^z(t)S_i^z(0) \rangle = 0.16(\hbar\omega_1/J) [\sin^2(\frac{1}{2}\omega_1 t)/\omega_1^2 t^2] + 0.0388h(t), \quad (21)$$

where $\omega_1 = 5.28J/\hbar$ and $h(t)$ is unity at $t=0$ and goes to zero as $t \rightarrow \infty$ at a rate t^{-1} or slower. The constant 0.0388 is chosen to make $\langle S_i^z(t)S_i^z(0) \rangle = \frac{1}{4}$ at $t=0$. The second derivative of the first term in (21) is $0.98J^2$ at $t=0$ which is very close to the exact value J^2 . Thus for short times, it is reasonable to use (21) with $h(t)=1$ since most of the variation comes from the first term. This, of course, is consistent with the idea that $\eta(\omega)$ in (20) should be negligible except for $\omega \gtrsim J/\hbar$. A plot of (21) with $h(t)=1$ is shown as curve (a) in Fig. 8. Windsor^{21(a)} has calculated correlation functions for linear chains of 4000 classical spins and times up to $t=6\hbar/2JS$. He has pointed out^{21(a)} that in order to compare his classical results with our quantum-mechanical ones for $S=\frac{1}{2}$, it is proper to take $S=\frac{1}{2}\sqrt{3}$ in his figures. This choice makes $S^2=\frac{3}{4}$, the quantum-mechanical value for $\mathbf{S} \cdot \mathbf{S}$. His curve for $\langle S_i^z(t)S_i^z(0) \rangle$, taking $S=\frac{1}{2}\sqrt{3}$, is shown as (b) in Fig. 8 and is seen to agree very well with our short-time behavior. He has also estimated the Fourier transform^{21(b)} of $\langle S_i^z(t)S_i^z(0) \rangle$ and finds it to be triangular for $\omega > 2JS/\hbar$ with, apart from a small tail, a cutoff at $5.37J/\hbar$ (for $S=\frac{1}{2}\sqrt{3}$) in close agreement with our figure $5.28J/\hbar$.

De Leener and Resibois¹⁷ have also estimated short-time behavior of $\langle S_i^z(t)S_i^z(0) \rangle$ by making approximations to their general theory. Their result is curve (c) of Fig. 8 and is seen to be in good agreement only for $Jt/\hbar \gtrsim 0.8$. In particular, they find it to pass through zero where no such behavior is indicated in our results or in Windsor's. It should be mentioned that they claim accuracy only for systems in which the number of exchange-coupled neighbors is large; so the linear chain is by no means a fair test of their methods.

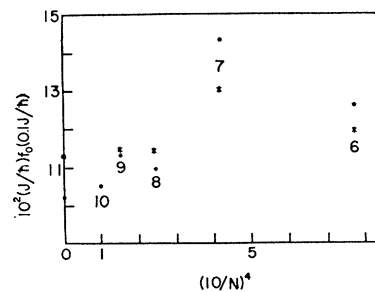


FIG. 7. Self-correlation function $f_0(\omega)$ in interval $0 \leq \omega < 0.2J/\hbar$ for varying N , as shown by numbers in vicinity of points. ●, closed chains; *, open chains. Points at $1/N=0$ are extrapolated values. This figure represents probably the worst case studied in terms of irregular behavior with N and difference between open and closed chain extrapolations.

²¹ (a) C. G. Windsor (private communication). (b) Windsor obtains Fourier transform by assuming $\langle S_i^z(t)S_i^z(0) \rangle$ to be proportional to $\sin(\pi t/t_1)/(\pi t/t_1)$ for $t > t_1$ with $t_1 = 6\hbar/2JS$. Behavior of $\langle S_i^z(t)S_i^z(0) \rangle$ for long times is not expected to alter critically the high-frequency part of the Fourier transform, upon which we base our comparison.

C. Wave-Vector Representation of Two-Spin Correlations

The spatial Fourier transform of two-spin time-correlation functions is pertinent to neutron scattering (2). We define $F_q(\omega)$ by

$$f_j(\omega) = N^{-1} \sum_q F_q(\omega) e^{-iqaj}, \quad (22)$$

where a is the lattice constant. Periodic boundary conditions and translational invariance restrict us to

$$qa = 2\pi n/N \quad (n = 0, 1, 2, \dots, N-1) \quad (23)$$

and lead to the relation

$$F_q(\omega) = \sum_{j=0}^N f_j(\omega) e^{iqaj}. \quad (24)$$

There are $\frac{1}{2}(N+1)$ different $f_j(\omega)$ for N odd and $\frac{1}{2}N$ different $f_j(\omega)$ for N even since $f_{j+N}(\omega) = f_j(\omega) = f_{-j}(\omega)$ for the closed chain. We see from (23) that it is not possible to get anything approaching long wavelengths ($qa \ll 1$) for the finite chains considered here. This is unfortunate since a good deal of theoretical work has focused on the long-wavelength limit and calculation of diffusion coefficients in this limit. The usual argument^{16,22,23} is that the diffusive character of $F_q(\omega)$ becomes important when

$$\langle \omega_q^4 \rangle / \langle \omega_q^2 \rangle^2 \gg 3,$$

where

$$\langle \omega_q^{2n} \rangle = \int_{-\infty}^{\infty} F_q(\omega) \omega_q^{2n} d\omega / \int_{-\infty}^{\infty} F_q(\omega) d\omega$$

is the $2n$ th moment and 3 is the Gaussian ratio. For a linear chain of spin- $\frac{1}{2}$ particles the general expression²⁴ reduces to

$$\langle \omega_q^4 \rangle / \langle \omega_q^2 \rangle^2 = \frac{1}{2} [(1 - \cos qa)^{-1} + 3]. \quad (25)$$

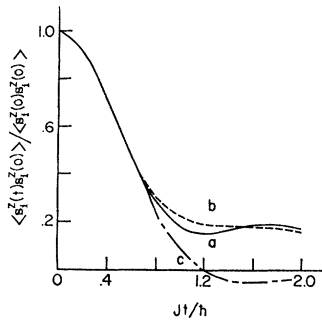


FIG. 8. Short-time behavior of $\langle S_i^z(t) S_i^z(0) \rangle$. Curve (a) — Eq. (21) with $h(t)=1$; curve (b) - - - Windsor's results (Ref. 21) for linear chain of classical spins and $S = \frac{1}{2}\sqrt{3}$ as explained in text; curve (c) - - - theory of De Leener and Resibois (Ref. 17).

²² P. G. De Gennes, J. Phys. Chem. Solids 4, 223 (1958).

²³ H. Mori and K. Kawasaki, Progr. Theoret. Phys. (Kyoto) 27, 529 (1962).

²⁴ M. F. Collins and W. Marshall, Proc. Phys. Soc. (London) 92, 390 (1967).

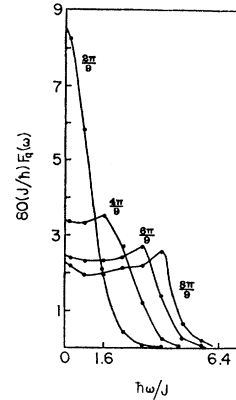


FIG. 9. Spatial Fourier transform $F_q(\omega)$ of two-spin correlation functions. Closed chain, $N=9$. Values of qa are $2n\pi/9$, $n=1, 2, 3, 4$, as indicated on figure. Solid curve for $2\pi/9$ is $8.5 \exp[-(\hbar\omega/1.34J)^2]$.

The smallest allowable qa for our finite chains is $\frac{1}{9}\pi$ which gives $\langle \omega_q^4 \rangle / \langle \omega_q^2 \rangle^2 \approx 4.1$; so at best we can get a ratio only about 30% higher than Gaussian. In fact, for all but the lowest nonzero qa , our ratios are less than the Gaussian limit.

Figure 9 shows $F_q(\omega)$ for $N=9$. At $qa = \frac{1}{9}\pi$, $F_q(\omega)$ is closely fitted by a Gaussian. This may not be too surprising since $\langle \omega_q^4 \rangle / \langle \omega_q^2 \rangle^2 = 3.64$ in this case which is not too far from the Gaussian value. Other $F_q(\omega)$ show a moderate peak at some nonzero ω followed by a rapid falloff. An essential postulate in the proof of Fernandez and Gersch¹⁹ on divergence of $f_j(\omega \rightarrow 0)$ is that $F_q(\omega)$ be a monotonically decreasing function of ω . This is certainly not the case for $qa \geq \frac{1}{9}\pi$. However, in their theory, divergence of $f_j(\omega \rightarrow 0)$ is associated with the long-wavelength behavior of $F_q(\omega)$, and there is nothing in our results to suggest (or deny) non-monotonic peculiarities as $q \rightarrow 0$.

A striking difference between $F_q(\omega)$ and $f_j(\omega)$ is that the former appears to be perfectly well behaved near $\omega=0$ for the q 's studied here. Because of this, it is possible to make reasonable estimates of $F_q(0)$ from the moments $\langle \omega_q^{2n} \rangle$, whereas such a procedure is not possible for $f_j(0)$.

D. Four-Spin Correlation Functions and Decoupling

Four-spin correlation functions are necessary for consideration of magnetic-resonance linewidth due to dipolar broadening. The Fourier transform of $\langle S_i^z(t) S_{i+1}^z(t) S_i^z(0) S_{i+1}^z(0) \rangle$ is shown in Fig. 10 for $N=9$. We note the following features. First, there is an apparent divergence at $\omega=0$ just as in the two-spin case. The two-spin divergence, however, is transparent from examination of the $q \rightarrow 0$ wave-vector components¹⁹ while the four-spin divergence is not, as we now demonstrate. Let K_q be given by

$$K_q = N^{-1/2} \sum_j S_j^z S_{j+1}^z e^{iqaj}. \quad (26)$$

Then we may write

$$\begin{aligned} \langle S_i^z(t) S_{i+1}^z(t) S_i^z(0) S_{i+1}^z(0) \rangle \\ = N^{-1} \sum_q \langle K_q(t) K_{-q}(0) \rangle, \end{aligned} \quad (27)$$

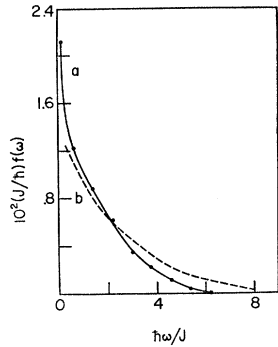


FIG. 10. Four-spin correlation function and decoupling approximation. Closed chain, $N=9$. Solid curve (a) is Fourier transform of $\langle S_i^z(t)S_{i+1}^z(t)S_i^z(0)S_{i+1}^z(0) \rangle$. Dashed curve (b) is decoupling approximation to this function, as explained in text.

where we have noted from translational invariance that

$$S_j^z S_{j+1}^z = N^{-1/2} \sum_q K_q e^{-iqaj} \quad (28)$$

and $\langle K_q(t)K_{q'}(0) \rangle = 0$ unless $q' = -q$, since

$$\langle S_i^z(t)S_{i+1}^z(t)S_j^z(0)S_{j+1}^z(0) \rangle$$

is a function only of $i-j$. If K_0 is a constant of the motion, then we might expect a divergence at $\omega=0$ in the Fourier transform of $\int dq \langle K_q(t)K_{-q} \rangle$, at least in one dimension where the long-wavelength modes contribute strongly to the integral. Such is the case for the two-spin correlations since the total spin is a constant of the motion. But K_0 does not commute with the exchange Hamiltonian (1) as is readily verified. Since the proof of Fernandez and Gersch¹⁹ makes use of the $q=0$ mode having an infinite lifetime, it is not applicable here. Thus, although Fig. 10 is as suggestive of a divergence at $\omega=0$ as are Figs. 3 and 4, there is no obvious long-wavelength reason why a divergence should occur, and perhaps some caution should be exercised in claiming an infinity at $\omega \rightarrow 0$. Other features of Fig. 10 are that the Fourier transform extends to higher frequencies than for two-spin correlations, and there is much less scatter in the points corresponding to interval centers.

With exact four-spin-correlation functions it is possible to examine the decoupling approximation

$$\langle S_i^z(t)S_{i+1}^z(t)S_i^z(0)S_{i+1}^z(0) \rangle \approx \langle S_i^z(t)S_i^z(0) \rangle^2 + \langle S_i^z(t)S_{i+1}^z(0) \rangle^2 \quad (29)$$

obtained from the general decoupling

$$\langle ABCD \rangle \approx \langle AB \rangle \langle CD \rangle + \langle AC \rangle \langle BD \rangle + \langle AD \rangle \langle BC \rangle \quad (30)$$

of spin operators A, B, C , and D which may be functions of time. Such decouplings are the basis of many theoretical treatments. Bennett and Martin,¹⁶ in particular, employ forms similar to (29) in their calculation of the diffusion coefficient at infinite temperature. If $f_{jk}(\omega)$

is the Fourier transform of

$$\langle S_i^z(t)S_{i+j}^z(0) \rangle \langle S_i^z(t)S_{i+k}^z(0) \rangle,$$

then we have

$$f_{jk}(\omega) = \int_{-\infty}^{\infty} d\omega' f_j(\omega') f_k(\omega - \omega'), \quad (31)$$

where $f_j(\omega')$ and $f_k(\omega - \omega')$ are defined by (16). Equation (29) and (31) are used together with the calculated two-spin functions to produce curve (b) in Fig. 10, which is the decoupling approximation to

$$\langle S_i^z(t)S_{i+1}^z(t)S_i^z(0)S_{i+1}^z(0) \rangle.$$

A zero-frequency divergence is not expected in $f_{jk}(\omega)$ unless the individual $f_j(\omega)$ and $f_k(\omega)$ go to infinity at a rate faster than or equal to $\omega^{-1/2}$ as $\omega \rightarrow 0$. Although the decoupling approximation is far from exact, it is fairly reasonable for $\omega \gtrsim J/\hbar$.

E. Temperature Dependence

Correlation functions have been computed as a function of temperature for antiferromagnetic ($J > 0$) coupling since this is the case of experimental interest. Figures 11 and 12 show temperature dependence of $f_0(\omega)$, $f_1(\omega)$, and $f_2(\omega)$ for the interval $-0.2J/\hbar \leq \omega < 0.2J/\hbar$ with $N=9$ and 10. Note that the curves for $N=9$ and 10 have very different behavior for $J/kT \gtrsim 0.2$. This is attributed to differences between even and odd numbers of spins on the chain in the limit $T \rightarrow 0$. Referring to Eq. (9) we see first that at zero frequency only degenerate states Φ_μ and Φ_ν contribute, and secondly Φ_μ is restricted to the ground state at $T=0$. For N even the antiferromagnetic ground state Φ_0 is nondegenerate and $\langle \Phi_0 | S_j^z | \Phi_0 \rangle = 0$. Hence $f_j(\omega \rightarrow 0)$ must go to zero as T goes to zero in even chains. But in odd chains the antiferromagnetic ground state is fourfold degenerate. Two of the degeneracies are associated with $S_z = \pm \frac{1}{2}$ while the other two come from the fact that the translation operator τ has a complex eigenvalue so that eigenfunctions both of τ and τ^* can be formed. It is therefore possible to have

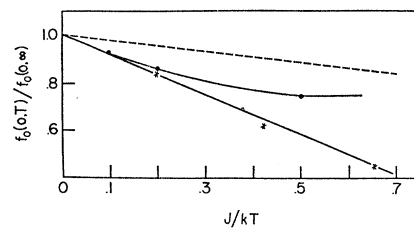


FIG. 11. Temperature dependence of near zero-frequency component $f_0(0, T)$ of self-correlation function normalized to its value at infinite temperature, $f_0(0, \infty)$. Points are for interval $-0.2J/\hbar \leq \omega < 0.2J/\hbar$. Closed chains \bullet , $N=9$; $*$, $N=10$. Dashed curve shows temperature dependence predicted by methods of moments and is explained in text. Coupling is antiferromagnetic.

nonzero $\langle \Phi_\mu | S_j^z | \Phi_\nu \rangle$ with Φ_μ and Φ_ν ground-state wave functions for N odd, and $f_j(\omega \rightarrow 0)$ need not vanish at zero temperature. Calculations for $J > kT$ (not shown here) confirm this difference between odd and even chains.

It is not, however, apparent to us why this zero-temperature difference should begin to manifest itself at temperatures as high as $5J/k$. A similar difference between odd and even chains occurs in the magnetic susceptibility which, for obvious reasons, goes to infinity in odd chains at $T=0$; but Bonner and Fisher⁶ find no significant difference between N even and odd for $T \gtrsim J/k$ (see Fig. 14 of Ref. 6).

We thus are not able to draw any conclusions about time correlations for temperatures below $5J/k$ and so cannot discuss the region in which the linear chain shows maxima in the specific heat and magnetic susceptibility. It does seem safe to conclude that $f_j(\omega \rightarrow 0)$ initially decreases as the temperature is lowered. For the self-correlation $f_0(\omega, T)$ this is in agreement with Richards' prediction²⁵ based on the Gaussian approximation and temperature dependence of ω_e (5). According to this we should have

$$\frac{f_0(0, T)}{f_0(0, \infty)} = \left(\frac{\langle [\mathcal{H}_C, [S_i^z]] S_i^z \rangle_\infty}{\langle [\mathcal{H}_C, [S_i^z]] S_i^z \rangle_T} \right)^{1/2} \equiv \frac{\omega_e(\infty)}{\omega_e(T)}, \quad (32)$$

where T and ∞ stand for values of quantities calculated at some finite temperature T and infinite temperature, respectively. In (32) we have noted that $\langle S_i^z S_i^z \rangle$ is independent of temperature so that, in the Gaussian approximation, all temperature dependence must be due to the effective frequency ω_e . The quantity $\omega_e(\infty)/\omega_e(T)$, as taken from Ref. 25, is shown as the dashed curve in Fig. 11. The variation is seen to be in the same direction as our calculated results but is much less pronounced. On a $1/T$ plot as given the initial slope of $f_0(0, T)/f_0(0, \infty)$ is about 4.5 times that of $\omega_e(\infty)/\omega_e(T)$.

Nearest- and next-nearest-neighbor correlation functions $f_1(\omega)$ and $f_2(\omega)$ have similar temperature dependence near zero frequency (Fig. 12). This is noteworthy because the areas under $f_1(\omega)$ and $f_2(\omega)$, $\langle S_i^z S_{i+1}^z \rangle$ and $\langle S_i^z S_{i+2}^z \rangle$, respectively, each increase in magnitude from zero as temperature is lowered and have different signs. Furthermore, the rate of change of $f_2(0)$ with temperature is almost identical to that of $f_0(0)$ and only about 50% less than that of $f_1(0)$. All this is in spite of the very different dependences of $\langle S_i^z S_i^z \rangle$, $\langle S_i^z S_{i+1}^z \rangle$, and $\langle S_i^z S_{i+2}^z \rangle$ on temperature. (The latter two static correlations are given in Fig. 12 while $\langle S_i^z S_i^z \rangle$ is constant.)

We conclude that for the linear chain there is no evident relation between temperature dependences of the near-zero-frequency part of $f_j(\omega)$ and the corresponding integral over all frequencies $\langle S_i^z S_{i+j}^z \rangle$.

²⁵ P. M. Richards, Phys. Rev. **142**, 196 (1966).

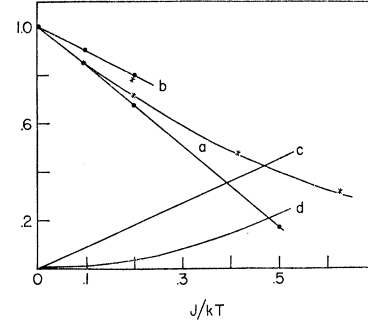


FIG. 12. Temperature dependence of nearest, f_1 , and next nearest, f_2 , neighbor correlation functions normalized to their values at infinite temperature. Points are for interval $-0.2J/\hbar \leq \omega < 0.2J/\hbar$. Closed chains \bullet , $N=9$; $*$, $N=10$. Curve (a): $f_1(0, T)/f_1(0, \infty)$, curve (b): $f_2(0, T)/f_2(0, \infty)$. For $N=9$ $f_1(0, T)$ changes sign at low temperatures; hence the different behavior with N for $f_1(0, T)$ and $f_0(0, T)$ (Fig. 11). Static correlations are also shown, normalized to their values at zero temperature (Ref. 6). Curve (c): $\langle S_i^z S_{i+1}^z \rangle / (-0.15)$, curve (d): $\langle S_i^z S_{i+2}^z \rangle / (0.0625)$. There is negligible difference between $N=9$ and $N=10$ for static correlations in temperature range shown.

Recently Silbernagel *et al.*²⁶ have assumed temperature dependence of $f_j(0)$ to be directly related to $\langle S_i^z S_{i+j}^z \rangle$ in describing temperature variation of NMR relaxation. Certainly our results negate their argument for the linear chain. It may be, though, that for three-dimensional systems, as they considered, such simple relations exist; and the effects we calculate here are all due to the divergence at $\omega=0$, which seems to become less severe at lower temperature.

IV. MAGNETIC-RESONANCE LINEWIDTH

We now apply the infinite temperature results of Sec. III to a calculation of frequency dependence of electron-spin-resonance linewidth in the linear chain salt CTS at infinite temperature. Exchange narrowing is assumed throughout so that the line is taken to be Lorentzian with a halfwidth at half maximum ΔH given by^{10,27}

$$\gamma \Delta H = (8\hbar^2 \langle M_x^2 \rangle)^{-1} \int_{-\infty}^{\infty} dt [\langle g^\dagger(t)g \rangle + \langle g(t)g^\dagger \rangle], \quad (33)$$

where γ is the magnitude of the gyromagnetic ratio. (For simplicity, we assume an isotropic gyromagnetic ratio for CTS. The effects of anisotropy on frequency dependence of ΔH are negligible.) M_x is the total x component of magnetization, and

$$g(t) = [\mathcal{H}_C(t), M_x + iM_y]. \quad (34)$$

In Eq. (34) \mathcal{H}_C is the dipolar Hamiltonian and time dependence is given by (4), but the Hamiltonian \mathcal{H} now includes a Zeeman part

$$\mathcal{H} = \mathcal{H}_{\text{ex}} - \gamma \hbar S_z H_0 \quad (35)$$

²⁶ B. G. Silbernagel, V. Jaccarino, P. Pincus, and J. H. Wernick, Phys. Rev. Letters **20**, 1091 (1968).

²⁷ The notation used here most closely follows that of P. M. Richards, Phys. Rev. **142**, 189 (1966).

for a field H_0 in the negative z direction. It is convenient to write \mathfrak{H}_1 as

$$\mathfrak{H}_1 = \sum_{M=-2}^2 G_M, \tag{36}$$

where

$$G_M(t) = e^{iM\omega_0 t} \hat{G}_M(t) \tag{37}$$

with

$$\hat{G}_M(t) = e^{i\mathfrak{H}_{\text{ex}} t / \hbar} G_M e^{-i\mathfrak{H}_{\text{ex}} t / \hbar} \tag{38}$$

and $\omega_0 = \gamma H_0$. Similarly, we have

$$g(t) = \sum_M \hat{g}_M(t) e^{iM\omega_0 t} \tag{39}$$

in which

$$\hat{g}_M(t) = [\hat{G}_M(t), M_x + iM_y]. \tag{40}$$

At infinite temperature $\langle g_{M'}^\dagger(t) g_{M'} \rangle = 0$ unless $M' = M$ so that we can write

$$\gamma \Delta H = \pi (2\hbar^2 \langle M_x^2 \rangle)^{-1} \sum_{M=-2}^2 J_M(M\omega_0), \tag{41}$$

where

$$J_M(\omega) = \frac{1}{2\pi} \int_{-\infty}^{\infty} dt e^{i\omega t} \langle \hat{g}_M^\dagger(t) \hat{g}_M \rangle, \tag{42}$$

and we have assumed infinite temperature so that $J_M(\omega) = J_M(-\omega)$ and $\langle \hat{g}_M^\dagger(t) \hat{g}_M \rangle = \langle \hat{g}_M(t) \hat{g}_M^\dagger \rangle$. Examination of the dipolar Hamiltonian gives the results¹⁸

$$J_0(\omega) = \sum_{ijkl} F_{ij}^{(0)} F_{kl}^{(0)} f_{ijkl}(\omega), \tag{43a}$$

$$J_1(\omega) + J_{-1}(\omega) = 10 \sum_{ijkl} F_{ij}^{(1)} F_{kl}^{(-1)} f_{ijkl}(\omega), \tag{43b}$$

$$J_2(\omega) + J_{-2}(\omega) = 4 \sum_{ijkl} F_{ij}^{(2)} F_{kl}^{(-2)} f_{ijkl}(\omega), \tag{43c}$$

where

$$F_{ij}^{(0)} = -\frac{3}{4} \gamma^2 \hbar^2 (3 \cos^2 \theta_{ij} - 1) r_{ij}^{-3}, \tag{44a}$$

$$F_{ij}^{(\pm 1)} = -\frac{3}{4} \gamma^2 \hbar^2 \sin \theta_{ij} \cos \theta_{ij} e^{\mp i \varphi_{ij}} r_{ij}^{-3}, \tag{44b}$$

$$F_{ij}^{(\pm 2)} = -\frac{3}{8} \gamma^2 \hbar^2 \sin^2 \theta_{ij} e^{\mp 2i \varphi_{ij}} r_{ij}^{-3}, \tag{44c}$$

$$F_{ii}^{(\pm M)} = 0 \tag{44d}$$

are the normal dipole factors with θ_{ij} and φ_{ij} the polar and azimuthal angles, respectively, the vector \mathbf{r}_{ij} between lattice sites i and j makes with respect to the z axis, and

$$f_{ijkl}(\omega) = \frac{1}{2\pi} \int_{-\infty}^{\infty} dt \langle S_i^+(t) S_j^+(t) S_k^-(0) S_l^-(0) \rangle e^{-i\omega t} \tag{45}$$

with $S_i^\pm = S_i^x \pm i S_i^y$. In (45) time dependence is given solely by \mathfrak{H}_{ex} , so the correlation function $f_{ijkl}(\omega)$ is directly related to the quantities we have calculated. For a rotationally invariant system—as is the case for expectation values at infinite temperature—it may be

shown that

$$\begin{aligned} & \langle [S_i^z(t) S_j^\pm(t) + S_i^\pm(t) S_j^z(t)] [S_k^z(0) S_l^\mp(0) \\ & \quad + S_k^\mp(0) S_l^z(0)] \rangle \\ & = 6 \langle [S_i^z(t) S_j^z(t) - \frac{1}{3} \mathbf{S}_i(t) \cdot \mathbf{S}_j(t)] \\ & \quad \times [S_k^z(0) S_l^z(0) - \frac{1}{3} \mathbf{S}_k(0) \cdot \mathbf{S}_l(0)] \rangle \\ & = \langle S_i^\pm(t) S_j^\pm(t) S_k^\mp(0) S_l^\mp(0) \rangle. \end{aligned} \tag{46}$$

Thus all the four-spin dipolar correlation functions may be reduced to $f_{ijkl}(\omega)$, a fact which has been used in Eqs. (43).

It is important to realize that although the exchange interaction is confined to spins within the same linear chain, the dipolar interaction is fully three dimensional. Hence the spins i, j, k , and l in

$$\langle S_i^+(t) S_j^+(t) S_k^-(0) S_l^-(0) \rangle$$

do not necessarily belong to the same chain. There are only two different nonzero possibilities: (1) i, j, k , and l belong to the same chain. In this case four-spin correlation functions similar to the one discussed in D of Sec. III are used. We have restricted the computations to cases where i is a neighbor of j , and k is a neighbor of l . Since the dipolar interaction falls off as a^{-3} and the correlations themselves decrease with distance, this should be an adequate approximation. (Note that we are concerned here with a one-dimensional dipolar sum since i, j, k , and l are confined to the same chain, and therefore rapid convergence is expected.) By translational invariance we may express the calculated four-spin correlation functions as

$$\langle S_1^+(t) S_2^+(t) S_j^-(0) S_{j+1}^-(0) \rangle$$

in which j runs from 1 to $\frac{1}{2}(N+1)$ for N odd and from 1 to $\frac{1}{2}(N+2)$ for N even in order to generate all the possible different correlations on a closed chain of N spins. The function $\langle S_1^+(t) S_2^+(t) S_j^-(0) S_{j+1}^-(0) \rangle$ is not in general simply related to $\langle S_1^z(t) S_2^z(t) S_j^z(0) S_{j+1}^z(0) \rangle$ so a separate calculation has to be made of longitudinal and transverse correlations. For $j=1$ it turns out that the two functions are almost identical while for $j>1$ there is noticeable difference. However, the $j=1$ function is close to an order of magnitude larger than $j>1$ functions for all frequency intervals studied. (2) i and k belong to one chain and j and l to another chain. Here time dependence of the pair i, k is independent of j, l since different chains are involved; so an exact decoupling

$$\begin{aligned} & \langle S_i^+(t) S_j^+(t) S_k^-(0) S_l^-(0) \rangle \\ & = \langle S_i^+(t) S_k^-(0) \rangle \langle S_j^+(t) S_l^-(0) \rangle \end{aligned} \tag{47}$$

may be made. The quantity $f_{ijkl}(\omega)$ is then given by integration of the two-spin correlations $f_{k-i}(\omega') \times f_{j-l}(\omega - \omega')$ in a manner analogous to (31). At infinite temperature

$$\langle S_i^+(t) S_k^-(0) \rangle = 2 \langle S_i^z(t) S_k^z(0) \rangle, \tag{48}$$

so that a separate calculation of transverse correlations is not necessary. In some cases they were calculated anyway to serve as a check on the program. Obviously if i and l belong to one chain and j and k to another, Eq. (47) holds with k and l interchanged. All other combinations give zero. For example, if i and j belong to one chain and k to l to another, then the function decouples to $\langle S_i^+(t)S_j^+(t) \rangle \langle S_k^-(0)S_l^-(0) \rangle = 0$; and if three indices belong to one chain and the fourth, say l , belongs to another chain, then l may be decoupled to give a result proportional to $\langle S_l^-(0) \rangle = 0$.

Eq. (43a) thus may be written as

$$J_0(\omega) = \sum_{ijkl}^{(1)} |F_{ij}^{(0)}|^2 f_{ijkl}(\omega) + 8 \sum_{ijkl}^{(2)} F_{ij}^{(0)} F_{kl}^{(0)} \int_{-\infty}^{\infty} f_{k-i}(\omega') f_{l-j}(\omega - \omega') d\omega', \quad (49)$$

where $\sum_{ijkl}^{(1)}$ means i, j, k , and l belong to the same chain, and i is a neighbor of j and k is a neighbor of l , according to our approximation discussed above, and where $\sum_{ijkl}^{(2)}$ means i and k belong to one chain and j and l belong to a different chain. The coefficient 8 multiplying $\sum_{ijkl}^{(2)}$ is the result of a factor of 4 arising from (48)—since f_{k-i} and f_{l-j} are two-spin z - z correlations—and a factor of 2 from the fact that an identical sum is obtained for i and l on one chain and j and k on another. Similar expressions are obtained from (43b) and (43c).

Operations indicated by (49) and like equations from (43b) and (43c) have been carried out for the CTS lattice²⁸ (Fig. 1) with $N=6-9$. For a given number of spins on the chain, the summations are truncated by the restriction that $f_{N/2}$ (N even) or $f_{(N+1)/2}$ (N odd) is the maximum two-spin correlation which can be computed for a closed chain of N spins, and f_{ijkl} is similarly limited as discussed above. Calculations were done both with H_0 along the a axis and along the c axis; it being assumed that the magnetic linear chains are in the direction of the c axis. Frequency dependence is essentially the same for the two cases, so only the a axis results (for which comparison can be made with experiment) are shown.

The resulting histogram, extrapolated to $N=\infty$, is given in Fig. 13. For comparison with experiment, J/k has been taken⁷ to be 3.15°K as inferred from specific heat and susceptibility data, and frequency is plotted in GHz instead of units of J/\hbar (when $\omega = J/\hbar$, $\omega/2\pi = 66 \times \text{GHz}$). On the same figure are shown Rogers experimental results^{11,12} at room temperature and the Gaussian approximation with $J/k=3.15^\circ\text{K}$. All points are normalized to 52.7 GHz ($\hbar\omega/J=0.8$) for convenience. The Gaussian approximation (5) reduces in this case to taking

$$\langle \hat{g}_M^\dagger(t) \hat{g}_M \rangle = \langle \hat{g}_M^\dagger \hat{g}_M \rangle e^{-\omega_e(M) t^2/2},$$

where we have noted that ω_e is not necessarily the same

²⁸ F. Mazzi, Acta Cryst. 8, 137 (1955).

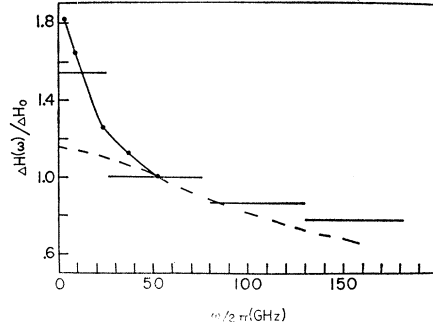


FIG. 13. Frequency dependence of linewidth in $\text{Cu}(\text{NH}_3)_4\text{SO}_4 \cdot \text{H}_2\text{O}$ at room temperature. ●, experimental points (Refs. 11 and 12). Horizontal lines are histogram values extrapolated to $N=\infty$. Dashed curve is Gaussian approximation [Eq. (50)]. All quantities have been normalized to 52.7 GHz, at which point $\Delta H = \Delta H_0$. Histogram points and Gaussian approximation are for $J/k = 3.15^\circ\text{K}$.

for each M , so it is written $\omega_e(M)$. We have calculated $\langle \hat{g}_M^\dagger \hat{g}_M \rangle$ and $\langle (d^2 \hat{g}_M^\dagger / dt^2)_{t=0} \hat{g}_M \rangle$ and obtained the result, for H_0 along the a axis,

$$\Delta H_{\text{Gaussian}} = 0.96(1 + 0.75 e^{-\omega^2/2\omega_e(1)^2} + 0.67 e^{-2\omega^2/\omega_e(2)^2}), \quad (50)$$

where ΔH is measured in oersteds, and $\omega_e(1) = 1.96 J/\hbar$ and $\omega_e(2) = 2.23 J/\hbar$. It is clear from the figure that the measured frequency dependence is completely out of line with the Gaussian approximation but is in accord with our computed correlation functions. A value, $J/k = 0.5^\circ\text{K}$, is required to fit the experimental points with a combination of Gaussians. Extrapolation of our results to $N=\infty$ is shown in Fig. 14 for the ratio $\Delta H(52.7 \text{ GHz})/\Delta H(13.2 \text{ GHz})$.

We calculate an absolute value $\Delta H = 4.8 \text{ Oe}$ at the interval centered at 13.2 GHz. Rogers' data fits $\Delta H = 8.6 \text{ Oe}$ at 13.2 GHz. [His measurements are of peak to peak width ΔH_{p-p} on a derivative curve and have been corrected for a Lorentzian by $\Delta H = (\sqrt{3}/2) \times \Delta H_{p-p}$]. The Gaussian approximation (50) gives $\Delta H = 2.3 \text{ Oe}$ at zero frequency. The measured ΔH is thus close to a factor of two greater than our calculated number. This is possibly due to contribution of interactions other than dipolar to the linewidth. Hyperfine coupling is expected²⁹ to contribute less than 1 Oe to

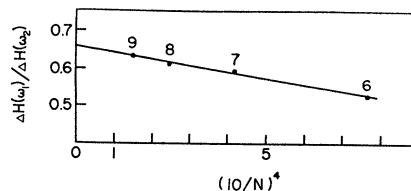


FIG. 14. Calculated linewidth for $N=6-9$ (closed chains) and extrapolation to $N=\infty$. Shown is ratio $\Delta H(\omega_1)/\Delta H(\omega_2)$, where $\omega_1 = 52.7 \text{ GHz}$, $\omega_2 = 13.2 \text{ GHz}$, and values are for intervals of widths 26.3 and 52.7 GHz centered at ω_2 and ω_1 , respectively. Frequencies are based on $J/k = 3.15^\circ\text{K}$.

²⁹ R. N. Rogers (private communication).

the low frequency ΔH , but anisotropic exchange may be important. Since similar correlation functions are involved, it is reasonable to expect that an additional spin-spin interaction would give a similar frequency dependence to that calculated here. We note¹⁴ that a discrepancy of about a factor of 2 also arises in the three-dimensional salt $\text{K}_2\text{CuCl}_4 \cdot 2\text{H}_2\text{O}$ between the measured ΔH and that calculated by Gaussian approximation. For this salt the Gaussian approximation gives satisfactory explanation of the frequency dependence.

V. SUMMARY AND CONCLUSIONS

Two-spin and four-spin time-correlation functions have been computed exactly for finite spin- $\frac{1}{2}$ Heisenberg linear chains containing up to 10 particles. The results are used to predict frequency dependence of electron spin resonance linewidth in the linear chain salt $\text{Cu}(\text{NH}_3)_4\text{SO}_4 \cdot \text{H}_2\text{O}$, and very good agreement is obtained with experiment. The frequency dependence of correlation functions and linewidth is most notably characterized by a sharp rise near zero frequency which makes a Gaussian approximation quite inadequate. This zero-frequency anomaly is *not* reflected in the density of states. From the high-frequency behavior of the self-correlation function an analytic expression is derived for the short-time behavior of $\langle S_i^z(t)S_i^z(0) \rangle$. This is found to agree well with calculations performed by Windsor on classical linear chains but not with the theory of Resibois and De Leener. The four-spin correlation function $\langle S_i^z(t)S_{i+1}^z(t)S_i^z(0)S_{i+1}^z(0) \rangle$ is computed and compared with the simple two-spin decoupling approximation, which is found to be fairly reasonable over a range of frequencies.

Temperature dependence of the two-spin correlation functions shows the near-zero frequency component to decrease as the temperature is lowered from an effectively infinite value to about $5J/k$. At temperatures below $5J/k$ results are inconclusive since different patterns emerge for odd and even numbers of spins on the chain.

Spatial Fourier analysis, useful for neutron scattering formulas, is made of the two-spin correlation functions. The wavelengths to which we are restricted by finite chains are far too short for anything to be said about the zero wave-vector limit. For short wavelengths $F_q(\omega)$ peaks at some nonzero frequency.

We conclude that finite chain calculations are reliable in predicting frequency dependence of correlation functions at infinite temperature. Our histograms are strongly suggestive of a divergence at zero frequency but, of course, do not prove it. Because of this zero-frequency behavior it is clear that predictions based on calculation of moments cannot be expected to be reliable for linear-chain problems, as is borne out by the ESR experiments.

It is natural to ask what insight can be gained into three-dimensional systems from results of this study.

The answer, we fear, is largely negative since the salient feature of our results, anomalous zero-frequency behavior, is likely to be strictly a dimensional effect, as discussed here and by Fernandez and Gersch.¹⁹ The high-frequency dependence of the self-correlation $f_0(\omega)$ which is triangular up to a certain frequency ($5.28 J/\hbar$ for the linear chain) and essentially zero above that, may, however, not be a dimensional effect. This, we feel, warrants further investigation. One positive note concerns applicability of classical spin-time-correlation functions. With classical spins it is possible to treat two- and three-dimensional systems with nearly as much accuracy as the linear chain since thousands of spins may be included. For quantum-mechanical matrix calculations as done here one is limited to not many more than 10 spins. This number may be sufficient to represent the infinite linear chain, but it cannot even include all next-nearest neighbors for a simple cubic lattice. Thus it is doubtful that our methods can meaningfully be extended to higher dimensions. But classical calculations^{21(a)} agree remarkably well with ours for the linear chain; and it is perhaps likely that this agreement between quantum and classical systems should continue into two and three dimensions. Hence the results of Windsor³⁰ and others³¹ on classical-time correlations in three dimensions may be considered as reliable in view of the accuracy noted here.

ACKNOWLEDGMENTS

Above all we wish to thank Mrs. P. M. Bauer and M. Subilia for programming and analyzing the open-chain calculations. Dr. C. G. Windsor kindly communicated his classical calculations and gave permission for their reproduction here. We have benefited greatly from discussion and correspondence with Dr. J. C. Bonner, Dr. M. E. Fisher, Dr. H. A. Gersch, Dr. R. B. Griffiths, Dr. G. Reiter, and Dr. R. N. Rogers. Computing was done with facilities of the University of Kansas Computation Center, whose staff is gratefully acknowledged.

APPENDIX: NUMERICAL NOTATION FOR SPIN STATES

In this section a numerical notation for the states of a linear chain is defined and the necessary algebra is developed in such a way that the problem of computing all possible states of the system, the action of arbitrary operators on these states, matrix elements, etc., is reduced to numerical operations which can be easily handled by the computer. Consider the states of a chain having r spins "up" and m spins "down" as a linear array of $r +$ signs and $m -$ signs. Let n_1 be the number of $-$ signs to the left of the first $+$ sign, n_2 the number of $-$ signs between the first and the second

³⁰ C. G. Windsor, Proc. Phys. Soc. (London) **91**, 353 (1967).

³¹ G. H. Vineyard, R. E. Watson, and M. Blume, J. Appl. Phys. **39**, 969 (1968).

+ signs, n_i the number of - signs between the $(i-1)$ th and the i th + signs, and n_{r+1} the number of - signs to the right of the last + sign in the chain. The set of numbers $(n_1, n_2, n_3, \dots, n_{r+1})$ can be used as a new representation of the given state. For example, the state $(- - + - + + - - + -)$ can be written $(2, 1, 0, 2, 1)$.

The representation defined above must satisfy the following two conditions:

- (a) For given N and r , there are $r+1$ numbers n .
- (b) $\sum_{i=1}^{r+1} n_i = m$.

We now consider the n 's as decimal digits of an integer number of $r+1$ digits, i.e., we form the number

$$\mathfrak{N} = n_1 \times 10^r + n_2 \times 10^{r-1} + \dots + n_r \times 10 + n_{r+1}. \quad (A1)$$

The number thus formed can be used to represent the given state. In the example above, the given state is represented by the number 21 021.

For given N and r , we have then the various states represented by a set of numbers \mathfrak{N} such that, according to condition (2), the sum of their digits is constant. From elementary arithmetic, we recall that numbers of this type can be obtained from one another by adding or subtracting multiples of nine. Using this property we shall see that the numbers representing the various states are connected by simple arithmetic operations.

With respect to condition (a), we may say that the set of numbers representing the states have the same number of digits if we conserve and count the zeros to the left of the first nonzero digit. For example the state

$$+ + - - + - \equiv 0021.$$

The advantage of this method is that the

$$\binom{N}{r}$$

different states having r spins reversed can be generated in numerical form starting from any given state. One way of doing this systematically is as follows: Start with the largest number of the set, i.e., the number $m \times 10^r$ which represents the state $(m, 0, 0, \dots, 0)$, and subtract $9 \times 10^{r-1}$ as many times as possible without violating condition (2), then subtract $9 \times 10^{r-2}$ from the numbers obtained in the first step, then subtract $9 \times 10^{r-3}$ and so on until we subtract 9 as many times as possible without violating condition (b). Each such subtraction gives a new state and the total number of such operations generates the

$$\binom{N}{r} - 1$$

states left.

An example will help to clarify the procedure. Consider a chain with $N=6$ and $r=2$. There are

$$\binom{6}{2} = 15$$

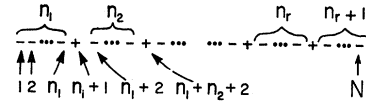


FIG. 15. Correspondence between numerical notation and orientation (+ or -) of spins.

states in this case. We start with the state

$$400 \equiv - - - - + +$$

and subtract first 90 and then 9 without violating (b). The required 15 numbers and operations performed are given in Table I. Note that all numbers are different and the sum of their digits is 4.

The states obtained when the operators of the problem act on any state given in numerical form can be found directly without recurring to the + and - notation. In order to show the procedure, we consider the correspondence between the two notations. First, we number the spins from 1 to N and refer to the j th spin as occupying the "position j ." When we refer to a pair of spins, one of which is at position i and the other at position j , we shall use the notation (i, j) to denote the pair. Consider the state $\mathfrak{N} \equiv (n_1, n_2, \dots, n_{r+1})$. The position number and the correspondence between the numerical notation and the + and - notation is as shown in Fig. 15.

The following rules are evident from examination of the diagram:

Rule 1: The k th + sign is at position

$$k + \sum_{i=1}^k n_i. \quad (A2)$$

Rule 2: (a) Every nonzero n_k (except n_1 and n_{r+1}) indicates a $(-+)$ pair at positions

$$(k-1 + \sum_{i=1}^k n_i, k + \sum_{i=1}^k n_i) \quad k=2, 3, \dots, r \quad (A3)$$

and a $(+-)$ pair at positions

$$(k-1 + \sum_{i=1}^{k-1} n_i, k + \sum_{i=1}^{k-1} n_i) \quad k=2, 3, \dots, r. \quad (A4)$$

TABLE I. Generation of numerical states for $N=6$ and $r=2$ by subtraction of 9 and 90 from basis state 400.

						-9→	
						400	
						310	
						301	
-90						220	202
↓						130	112
						040	031
							103
							022
							013
							004

TABLE II. Relations between n_1, n_{r+1} and orientation of spins.

		There is a (-+) pair at	There is a (+-) pair at
$n_1 \neq 0$	$n_{r+1} \neq 0$	(n_1, n_1+1)	$(N-n_{r+1}, N-n_{r+1}+1)$
	$n_{r+1} = 0$	(n_1, n_1+1)	$(N, 1)$
$n_1 = 0$	$n_{r+1} \neq 0$	$(N, 1)$	$(N-n_{r+1}, N-n_{r+1}+1)$
	$n_{r+1} = 0$	There are no opposite-sign pairs other than those stated in (a).	

(b) Relations with respect to n_1 and n_{r+1} are given in Table II.

A. Translation Operator

When dealing with closed chains or “rings” it is convenient to define a translation operator τ which translates spins to the left, i.e., for example, for $N=6, r=3$, and in particular the state $(--++--)$ we have

$$\tau(--++--)=(-++-+-).$$

In general, if we act with this operator N times on a given state we obtain the original state back.

In terms of our numerical notation, the action of τ on a given state is found by subtracting from \mathfrak{X} the number 10^r-1 . For example, $310 \equiv ----++-$

$$\tau(310) = 310 - 99 = 211 \equiv ---+-+--.$$

The set of all translations of a given state is obtained by subtracting 10^r-1 as many times as possible. Each one of these operations gives a new translation state. When the next subtraction is not possible, we multiply the last number obtained by 10 (this operation gives a new translation state) and repeat the procedure until we get the initial number again. An example is shown in Table III.

We may see how this occurs by noting first that

$$\tau(n_1, n_2, \dots, n_{r+1}) = (n_1-1, n_2, \dots, n_{r+1}+1), \text{ if } n_1 \neq 0 \quad (A5)$$

$$\tau(0, n_2, \dots, n_{r+1}) = (n_2, n_3, \dots, n_{r+1}, 0), \text{ if } n_1 = 0. \quad (A6)$$

In the form of Eq. (A1) we can write

$$\begin{aligned} & (n_1-1) \times 10^r + n_2 \times 10^{r-1} + \dots + n_{r+1} + 1 \\ & = n_1 \times 10^r + n_2 \times 10^{r-1} + \dots + n_{r+1} - (10^r - 1), \\ & n_2 \times 10^r + n_3 \times 10^{r-1} + \dots + n_{r+1} \times 10 \\ & = (n_2 \times 10^{r-1} + n_3 \times 10^{r-2} + \dots + n_{r+1}) \times 10 \end{aligned}$$

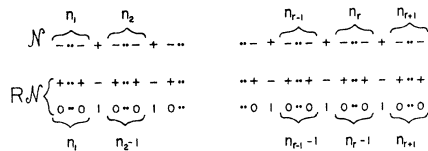


FIG. 16. Diagrammatic representation of action of rotation operator R on numerical state \mathfrak{X} .

TABLE III. Generation of translations of the state 310. “Operation” refers to the operation performed on the state in the same row to produce the state in the row beneath.

State	Operation	Equivalence
310	-99	---++--
211	-99	---+-+--
112	-99	---+--
013	$\times 10$	+-+---
130	-99	+-+---
031	$\times 10$	+---+--
310		

for the two cases given by (A5) and (A6), respectively. Then, we see that the multiplication by 10 comes when n_1 becomes zero.

B. Rotation Operator

Further reduction of the order of the matrices in exact calculations on linear chains is obtained by defining a rotation operator, R , which transforms a spin “up” into a spin “down” and vice versa, i.e., for example

$$R(+--+)=(-+--).$$

In numerical notation, the action of R on the state $\mathfrak{X} \equiv (n_1, n_2, \dots, n_{r+1})$ is described by the formula

$$R\mathfrak{X} = 10^{n_1+n_2+\dots+n_{r+1}} + 10^{n_3+\dots+n_{r+1}} + \dots + 10^{n_r+n_{r+1}} + 10^{n_{r+1}} \quad (A7)$$

$$= \sum_{\alpha=2}^{r+1} 10 \sum_{i=\alpha}^{r+1} n_i.$$

Example:

$$\begin{aligned} R(+--+)=R(0210) \\ = 10^{2+1+0} + 10^{1+0} + 10^0 = 1011 \\ \equiv -++-+- \end{aligned}$$

Equation (A7) can be proved by means of the diagram in Fig. 16 where we have written the original state \mathfrak{X} and below it the resulting state $R\mathfrak{X}$ in both + and - notation and number notation. Note that $R\mathfrak{X}$ has $m+1$ digits, provided we count the n_1 zeros to the left of the first nonzero digit. If the state has $r = m = \frac{1}{2}N$ (even N), we have that \mathfrak{X} and $R\mathfrak{X}$ have the same number of digits.

C. Reflection Operator

For open chains we make use of an operator P which reflects all spins about the midpoint. (With N odd, P leaves the spin at lattice point $\frac{1}{2}(N+1)$ unchanged.) Since P produces a state in which the left-right order of spins up and down is replaced by right-left order, it is evident that

$$\begin{aligned} P(n_1, n_2, n_3, \dots, n_{r-1}, n_r, n_{r+1}) \\ = (n_{r+1}, n_r, n_{r-1}, \dots, n_3, n_2, n_1). \quad (A8) \end{aligned}$$

D. Exchange Hamiltonian

Action of the exchange Hamiltonian (1) on arbitrary states can be described in numerical form as follows. Consider first the operator

$$\sum_{i=1}^N (S_i^+ S_{i+1}^- + S_i^- S_{i+1}^+),$$

with condition $S_{N+1}^\pm = S_1^\pm$. The action of this operator on a given state \mathfrak{X} is equal to a sum of states of the form: $\mathfrak{X} \pm 9 \times 10^{r-1}$, $\mathfrak{X} \pm 9 \times 10^{r-2}$, ..., $\mathfrak{X} \pm 9$, $10(\mathfrak{X} + 10^{r-1} - 1)$, and $(\mathfrak{X}/10) + 1 - 10^{r-1}$. This sum consists of only those terms which do not violate condition (b).

Example: Suppose $\mathfrak{X} = 310 \equiv ---+-+$.

$$\begin{aligned} S_i^+ S_{i+1}^-(n_1, \dots, n_{r+1}) &= (n_1, \dots, n_k - 1, n_{k+1} + 1, \dots, n_{r+1}), \text{ if } n_k \neq 0 \text{ and } i = k - 1 + \sum_{l=1}^k n_l \quad k = 1, 2, \dots, r, \\ &= (n_2 + 1, n_3, \dots, n_{r+1} - 1, 0), \text{ if } n_1 = 0, n_{r+1} \neq 0 \text{ and } i = N \\ &= 0, \text{ otherwise.} \end{aligned}$$

$$\begin{aligned} S_i^- S_{i+1}^+(n_1, \dots, n_{r+1}) &= (n_1, \dots, n_{k-1} + 1, n_k - 1, \dots, n_{r+1}), \text{ if } n_k \neq 0 \text{ and } i = k - 1 + \sum_{l=1}^k n_l \quad k = 2, 3, \dots, r + 1, \\ &= (0, n_1 - 1, n_2, \dots, n_{r+1}), \text{ if } n_{r+1} = 0, n_1 \neq 0 \text{ and } i = N \\ &= 0, \text{ otherwise.} \end{aligned}$$

Summing over i we obtain the following equations:

$$\begin{aligned} \sum_{i=1}^N S_i^+ S_{i+1}^-(n_1, \dots, n_{r+1}) &= \sum_{k=1}^r (1 - \delta_{n_k, 0})(n_1, \dots, n_k - 1, n_{k+1} + 1, \dots, n_{r+1}) \\ &\quad + (1 - \delta_{n_{r+1}, 0}) \delta_{n_1, 0} (n_2 + 1, n_3, \dots, n_{r+1} - 1, 0), \end{aligned} \tag{A9a}$$

$$\begin{aligned} \sum_{i=1}^N S_i^- S_{i+1}^+(n_1, \dots, n_{r+1}) &= \sum_{k=1}^{r+1} (1 - \delta_{n_k, 0})(n_1, \dots, n_{k-1} + 1, n_k - 1, \dots, n_{r+1}) \\ &\quad + (1 - \delta_{n_1, 0}) \delta_{n_{r+1}, 0} (0, n_1 - 1, n_2, \dots, n_{r+1}). \end{aligned} \tag{A9b}$$

Now,

$$\begin{aligned} \mathfrak{X} &\equiv (n_1, n_2, \dots, n_{k-1}, n_k, n_{k+1}, \dots, n_{r+1}) \\ &= n_1 \times 10^r + \dots + n_{k-1} \times 10^{r-k+2} + n_k \times 10^{r-k+1} + n_{k+1} \times 10^{r-k} + \dots + n_{r+1}, \end{aligned}$$

therefore, the k th state in (A9a) is found by subtracting $9 \times 10^{r-k}$ from \mathfrak{X} , since

$$\begin{aligned} (n_k - 1) \times 10^{r-k+1} + (n_{k+1} + 1) \times 10^{r-k} &= n_k \times 10^{r-k+1} \\ &\quad + n_{k+1} \times 10^{r-k} - (10 - 1) \times 10^{r-k}, \end{aligned}$$

and the k th state in (A9b) is found by adding $9 \times 10^{r-k+1}$ to \mathfrak{X} , since

$$\begin{aligned} (n_{k-1} + 1) \times 10^{r-k+2} + (n_k - 1) \times 10^{r-k+1} &= n_{k-1} \times 10^{r-k+1} \\ &\quad + n_k \times 10^{r-k+1} + (10 - 1) \times 10^{r-k+1}. \end{aligned}$$

For the last state in (A9a) we have $\mathfrak{X} = n_2 \times 10^{r-1} + n_3 \times 10^{r-2} + \dots + n_{r+1}$, since it exists only if $n_1 = 0$. Then,

$$\begin{aligned} (n_2 + 1) \times 10^r + n_3 \times 10^{r-1} + \dots + (n_{r+1} - 1) \times 10 \\ = 10(\mathfrak{X} + 10^{r-1}). \end{aligned}$$

For the last state in (A9b), $\mathfrak{X} = n_1 \times 10^r + n_2 \times 10^{r-1}$

The terms which do not violate condition (b) are

$$\begin{aligned} \mathfrak{X} + 9 \times 10^{r-1} &= 310 + 90 = 400 \equiv ----+ +, \\ \mathfrak{X} - 9 \times 10^{r-1} &= 310 - 90 = 220 \equiv ---+---+, \\ \mathfrak{X} - 9 \quad 10^{r-2} &= 310 - 9 = 301 \equiv ----+ +- , \\ (\mathfrak{X}/10) + 1 - 10^{r-1} &= 031 + 1 - 10 = 022 \equiv +---+---. \end{aligned}$$

Therefore, we have

$$\begin{aligned} \sum_{i=1}^N (S_i^+ S_{i+1}^- - S_i^- S_{i+1}^+) &(310) \\ &= (400) + (220) + (310) + (022). \end{aligned}$$

To verify the procedure, we consider first the operators $S_i^+ S_{i+1}^-$ and $S_i^- S_{i+1}^+$. Using rule 2 we have

$+\dots+n_r \times 10$, since it exists only if $n_{r+1} = 0$. In this case we have

$$\begin{aligned} (n_1 - 1) \times 10^{r-1} + n_2 \times 10^{r-2} + \dots + n_{r+1} + 1 \\ = (\mathfrak{X}/10) + 1 - 10^{r-1}. \end{aligned}$$

The requirement that $n_k \neq 0$ for the existence of the k th state in Eqs. (A9) is equivalent to the statement that condition (b) must not be violated when we add or subtract the required quantities.

Action of the operator $\sum_{i=1}^N S_i^z S_{i+1}^z$ with $S_{N+1}^z = S_1^z$ is described by the formula

$$\begin{aligned} \sum_{i=1}^N S_i^z S_{i+1}^z \mathfrak{X} \\ = \frac{1}{4} [N - 4d_0 + 4(1 - \delta_{n_1, 0})(1 - \delta_{n_{r+1}, 0})], \end{aligned} \tag{A10}$$

where $\mathfrak{X} \equiv (n_1, n_2, \dots, n_{r+1})$ and d_0 is equal to the number

of nonzero n 's in \mathcal{N} . Equation (A10) is a direct consequence of rule 3.

Examples:

$$\sum_{i=1}^N S_i^z S_{i+1}^z (310) = \frac{1}{4} [6 - (4 \times 2)] (310) = -\frac{1}{2} (310),$$

$$\sum_{i=1}^N S_i^z S_{i+1}^z (301) = \frac{1}{4} [6 - (4 \times 2) + 4] (301) = \frac{1}{2} (301).$$

The chain of largest number of spins that we can treat using this numerical method depends on the

maximum number of digits that a particular computer can handle. On the other hand, the application of the method is limited by the fact that none of the n 's can have a value larger than 9. Since the matrix elements with respect to states having z component of total spin $S_z = M$ or $S_z = -M$ are identical, we have to deal only with half the total matrix, i.e., with values $m = \frac{1}{2}N$, $r = \frac{1}{2}N$. Therefore, the method is limited to a maximum of 18 spins in the chain, which is a larger number than can be handled by present day computers since 18 spins would require diagonalization of matrices of the order of 4800×4800 .

Direction of Easy Magnetization in Gadolinium

FREDERICK MILSTEIN

The Rand Corporation, Santa Monica, California 90406

AND

LAWRENCE BAYLOR ROBINSON*

University of California, Los Angeles, California 90024

(Received 19 February 1968)

The direction of easy magnetization in Gd is studied as a function of temperature and pressure. The pertinent experimental results have already been given by Robinson, Milstein, and Jayaraman. A Gd sample was used as the core of a small transformer; a constant input voltage was supplied to this transformer. The secondary voltage was monitored as a function of temperature at several constant pressures. The secondary voltage of the transformer, being proportional to the permeability of the sample, is a sensitive indicator of changes in magnetic structure in the Gd sample. Typically, the secondary voltages behave as follows as the temperature of the transformer is lowered: A sharp rise in the secondary voltage occurs at the Curie temperature, followed by another sharp rise at a temperature well below the Curie point. The magnitude of the secondary voltage at this latter transition is from two to three orders of magnitude greater than at the transition from the paramagnetic to the ferromagnetic state. This transition is interpreted as a magnetic transition in which the direction of easy magnetization in Gd deviates from the c axis. The angle of deviation is discussed in terms of the (small) anisotropy constants resulting from the weak crystalline field in Gd. In terms of the output voltage, one is able to obtain the relative deviations of the direction of easy magnetization from the c axis. The temperatures, as a function of pressure, at which the maximum deviations occur can also be obtained. As the temperature is lowered further, the direction of easy magnetization starts to approach the c axis again. Comparisons are made with other measurements of this angle of deviation.

INTRODUCTION

IN an earlier paper¹ we presented the results of a study undertaken primarily to determine the dependence of the Curie temperature of gadolinium (Gd) metal upon pressure. Figure 1 is one of the curves that appeared in the earlier paper (it was then numbered Fig. 5). The experimental details are discussed in Ref. 1. Briefly, a Gd sample was used as the core of a small transformer, the secondary voltage, e_0 , of which was monitored as a function of temperature at several

constant pressures. Since the secondary voltage is proportional to the permeability of the sample, it serves as a sensitive indicator of changes in the magnetic structure of the sample. Hence, for example, e_0 increases sharply at the Curie point T_C where the sample transforms from the paramagnetic to the ferromagnetic state.

The principal effects observed in Fig. 1 are summarized as follows:

- (a) The Curie temperature T_C decreases with increasing pressure as shown by the shift with pressure of the initial increase in secondary voltage. This effect occurs in temperatures ranging from about 250 to 293°K. (Data taken in this temperature range are published as Fig. 3 of Ref. 1.)

* Part of this work was completed when one of us (L.B.R.) held a John Simon Guggenheim Memorial Fellowship.

¹L. B. Robinson, F. Milstein, and A. Jayaraman, Phys. Rev. **134**, A187 (1964).